Theoretical Calculation of $ClONO_2$ and $BrONO_2$ Bond Dissociation Energies

Peng Zou, Agnes Derecskei-Kovacs, and Simon W. North*

Chemistry Department, Texas A&M University, P. O. Box 30012, College Station, Texas 77842

Received: August 27, 2002; In Final Form: November 19, 2002

CCSD(T) basis set limit bond dissociation energies by extrapolation for $ClONO_2$ and CCSD(T)/cc-pV5Z estimates of bond dissociation energies for $BrONO_2$ were calculated by determining correction factors to MP2/cc-pVXZ (X = 2−5) basis set energies. To obtain the MP2 basis set limit energies, MP2/cc-pVXZ (X = 2−5) level calculations were extrapolated to the basis set limit using either polynomial or exponential functional forms. Correlation effects were taken into account by calculating the difference in energies at the MP2/cc-pVTZ and CCSD(T)/cc-pVTZ levels. Subsequent corrections for the spin−orbit energy of the atomic fragment and zero point energy were applied to yield the final bond dissociation energies. The theoretical results are in good agreement with available experimental values and theoretical values calculated using isodesmic methods.

I. Introduction

Chlorine nitrate ($ClONO_2$) and bromine nitrate ($BrONO_2$) are two major temporary reservoirs for active chlorine and bromine in the stratosphere and, as such, play an important role in stratospheric ozone chemistry.[1−4] It is therefore not surprising that numerous studies have been performed to understand the chemistry of these two compounds.[5−12] Their formation occurs primarily through the recombination of XO and NO_2. The removal processes involve photolysis and heterogeneous reactions, the latter during low sun conditions in the polar region. There are several photolysis channels that can be accessed in stratosphere

$$XONO_2 \xrightarrow{h\nu} X + ONO_2 \quad (1)$$

$$XONO_2 \xrightarrow{h\nu} XO + NO_2 \quad (2)$$

$$XONO_2 \xrightarrow{h\nu} XONO + O \quad (3)$$

However, because the dominant thermal dissociation products are XO + NO_2, the XO−NO_2 bond energies remain the only bond energies that have been determined experimentally. An accurate assessment of the remaining bond energies is important for a detailed understanding of both thermal chemistry and photochemistry of halogen nitrates.

The $ClONO_2$ heat of formation has been measured to high accuracy by extensive laboratory studies,[13−18] and the ClO−NO_2 bond energy has been accurately derived using the experimental heats of formation for ClO and NO_2. Anderson and Fahey have analyzed the previous results and reported a ClO−NO_2 bond energy of 26.65 ± 0.1 kcal/mol at 298 K.[18] Orlando and Tyndall have recently measured the thermal decomposition rates of $BrONO_2$ to give BrO and NO_2.[19] On the basis of the recombination rates recommended by NASA panel,[20] they determined the $BrONO_2$ heat of formation at 298 K to be 9.7 ± 2.0 kcal/mol and the BrO−NO_2 bond strength to be 28.2 ± 1.5 kcal/mol.

There have been several theoretical studies on the equilibrium structure, harmonic frequencies, and heats of formation of ground state chlorine and bromine nitrate.[21,22] Lee has calculated the equilibrium structure, vibrational frequency, and dipole moment of $ClONO_2$ by using the singles and doubles coupled cluster method that also includes a perturbational estimation of the effects of connected triple excitations, CCSD(T), with a triple-ζ double-polarized basis set, TZ2P.[21] The results show excellent agreement with experimental data. Because the heat of formation of $ClONO_2$ is known to high accuracy from experiment, no calculation was been performed to determine this value by the author. Similarly, the equilibrium structure and vibrational frequencies of $BrONO_2$ have been calculated by Parthiban and Lee at the CCSD(T)/TZ2P level and are also in excellent agreement with experimental results.[22] The heat of formation of $BrONO_2$ is predicted to be 10.1 kcal/mol using two isodesmic reactions. This result is in excellent agreement with experimental result by Orlando and Tyndall.[19] In a subsequent theoretical study of $XONO_2$ (X = Br, OBr, O_2Br) by Parthiban and Lee,[23] density functional theory (DFT) was used to determine the equilibrium geometry, dipole moment, and harmonic frequencies. The B3LYP hybrid functional and TZ2P basis sets were used in their calculations. The B3LYP/TZ2P results of $BrONO_2$ are in good agreement with experimental data and their previous CCSD(T)/TZ2P results.

Lee and co-workers also performed theoretical calculations on ClONO and BrONO at the CCSD(T)/TZ2P level.[24,25] ClONO and BrONO are photodissociation products of $ClONO_2$ and $BrONO_2$ (channel 3) and may also be derived from the bimolecular reactions Br + NO_2 or BrO + NO. The CCSD(T)/TZ2P harmonic vibrational frequencies agree well with available experimental data for isomers of both ClONO and BrONO. Calculations with large atomic natural orbital basis sets at the CCSD(T) level predict that the cis isomer is more stable than the trans isomers for both ClONO (3.1 ± 0.8 kcal/mol) and BrONO (3.7 ± 1.0 kcal/mol).

In all previous studies, bond energies were derived from the isodesmic methods, which inherit the experimental uncertainties from the heats of formation of all of the species involved in the isodesmic reactions. We have performed direct bond energy calculations for $ClONO_2$ and $BrONO_2$ at the coupled cluster

* To whom correspondence should be addressed. E-mail: north@mail.chem.tamu.edu.

10.1021/jp021961y CCC: $25.00
Published on Web 01/21/2003

TABLE 1: Correlation and Basis Set Effects on the Calculated Equilibrium Geometry of $BrONO_2$ (Distances in Ångstroms and Angles in Degrees)

method and basis set	r(Br−O)	r(O−N)	r(N−O_{cis})	r(N−O_{trans})	α(Br−O−N)	α(O−N−O_{cis})	α(O−N−O_{trans})
MP2(full)/cc-PVTZ[b]	1.810	1.511	1.187	1.190	112.6	117.2	108.4
MP2(FC14)/cc-PVTZ[c]	1.820	1.519	1.191	1.194	112.7	117.3	108.3
MP2(FC8)/cc-PVTZ[d]	1.814	1.522	1.191	1.194	112.5	117.2	108.2
MP2/6-311++G*	1.854	1.524	1.193	1.195	113.4	117.6	108.1
MP2/6-311++G(3df)	1.821	1.502	1.190	1.193	113.0	117.4	108.6
B3LYP/6-311+G*	1.866	1.483	1.192	1.193	115.6	118.2	109.0
B3LYP/cc-PVTZ	1.843	1.482	1.189	1.191	115.2	118.1	110.0
B3LYP/aug-cc-PVTZ	1.837	1.484	1.189	1.191	115.1	118.0	109.2
B3LYP/6-311++G(3df)	1.838	1.478	1.188	1.190	115.1	118.0	109.2
experiment[a]	1.829	1.456	1.205	1.205	113.9	119.5	106.6

[a] Ref 32. [b] All electrons correlated. [c] 1s,2sp,3sdp orbitals of Br atom frozen. [d] 1s,2sp,3sp orbitals of Br atom frozen.

level with single and double excitations using triple excitations perturbatively (CCSD(T)) in conjunction with the Dunning correlation consistent basis sets. The procedure involves the calculation of bond dissociation energies for $ClONO_2$ and $BrONO_2$ with a large number of basis sets and different levels of electron correlation. The Moller−Plesset (MP2) results with correlation consistent polarized valence basis set are then extrapolated to the infinite basis set limit with either an exponential or a polynomial functional form. An approximation to the CCSD(T) bond energy at the infinite basis set limit can be obtained by applying a correlation correction factor to MP2 results in order to estimate the CCSD(T) results. We find that the calculated bond energies of $ClONO_2$ and $BrONO_2$ are in good agreement with experimental values where available. Finally, density functional methods were also employed to determine the bond energies, and they are compared with the ab initio results.

II. Results and Discussion

A. Geometry Calculations. We have performed geometry optimizations using second-order Moller−Plesset (MP2) approximation and the B3LYP methods[26,27] with a large number of different Pople style (6-31xG)[28,29] and correlation consistent polarized valence (cc-pVXZ)[30,31] basis sets for $BrONO_2$ in order to ascertain the appropriate level of theory. Shown in Table 1 are the results of geometry optimizations at different levels and the experimental values for comparison. The geometry of $BrONO_2$ was constrained to be planar since both experimental[32] and our unconstrained results show the assumption to be valid for this compound.

Role of the Size of the Frozen Core. The correlation consistent basis sets for fourth row elements were originally optimized by only correlating the 4sp-like valence molecular orbitals. Because this is different from the Gaussian 98 default setting, to evaluate the effect of the frozen core approximation on geometry optimizations using MP2, the $BrONO_2$ geometry was optimized by using the cc-pVTZ basis set with different sizes of the frozen core in the Br atom, i.e., full (all electrons correlated); fc14 option (1s,2sp,3sdp orbitals frozen), and fc8 (1s,2sp,3sp orbitals frozen). For O and N atoms, frozen core orbitals only include 1s-like core molecular orbitals. Although the difference between the different sizes of frozen core is subtle, it is not surprising to see that the fc14 results are closer to the experimental results, since the cc-pVTZ basis set is optimized for calculations involving only 4sp-like valence molecular orbitals.

Role of the Computational Model. In general, the optimized geometries at the MP2 and B3LYP levels are quite close to each other using the same basis set except for the $BrO-NO_2$ bond length. When the same basis set is used, MP2 calculations usually overestimate the $BrO-NO_2$ bond length. Even at the MP2/6-311++G(3df) level, the calculated $BrO-NO_2$ bond is still ∼0.05 Å longer than the experimental result, while the B3LYP/6-311++G(3df) $BrO-NO_2$ bond length is more accurate resulting in a deviation from experiment of only 0.02 Å.

Role of the General Type of the Basis Set. The correlation consistent cc-pVTZ basis set appears to slightly underperform the Pople style 6-311++G(3df) basis set in the geometry optimization of the $BrONO_2$ molecule. At the MP2 level of theory (fc14), the $Br-ONO_2$ bond lengths are fairly close to experiment using the two basis sets, but the $BrO-NO_2$ bond length with the cc-pVTZ basis set is 0.017 Å longer than the 6-311++G(3df) result. At the B3LYP level of theory, both the $Br-ONO_2$ and the $BrO-NO_2$ bond lengths are longer when the cc-pVTZ basis set is used. In the presence of augmentation (aug-cc-pVTZ), the $Br-ONO_2$ bond length is only slightly improved, while the $BrO-NO_2$ bond length is even worse. On this basis, the 6-311++G(3df) basis set was adopted for further geometry optimizations based on the $BrONO_2$ results. It should be noted that although our B3LYP/6-311++G(3df) geometry of $BrONO_2$ is in excellent agreement with Parthiban and Lee's CCSD(T)/TZ2P calculation, both results of the $Br-ONO_2$ and $BrO-NO_2$ bond lengths are longer than the experimental data,[22] which indicates a need for more accurate experimental or theoretical determination. It is worth noting that the geometry is greatly improved in the presence of more accurate polarization functions in the basis set at both the MP2 and the B3LYP levels of theories by comparing the results of the 6-311++G* and 6-311++G(3df) basis sets. The improvement is especially pronounced for the $Br-ONO_2$ and $BrO-NO_2$ bond lengths. At the B3LYP level of theory, the $Br-ONO_2$ bond lengths are 1.866 and 1.838 Å with the 6-311++G* and 6-311++G(3df) basis sets, respectively, while the $BrO-NO_2$ bond lengths are 1.483 and 1.478 Å. The (BrONO)−O bond lengths only change slightly in the presence of better polarization functions, indicating that there is a stronger effect on the Br atom than on the much lighter N and O atoms. An earlier study of the $BrONO_2$ molecular geometry at the B3LYP/6-311G(d) level also predicted a longer $Br-ONO_2$ bond length relative to experiment.[33]

Geometry optimizations with the 6-311++G(3df) basis set using both MP2 and B3LYP were performed for $ClONO_2$, ClO, and BrO as well (only $ClONO_2$ results are shown in Table 2). The $ClO-NO_2$ bond length at the MP2 level and B3LYP level is 0.049 and 0.013 Å longer than the experimental result, respectively. The (ClONO)−O bond lengths predicted by the B3LYP and MP2 methods are very similar. For the bond angles in the $ClONO_2$ molecule, B3LYP results are in much better agreement with experimental data than the MP2 results. The B3LYP/6-311++G(3df) calculations somewhat overestimated the X−O (X = Br, Cl) bond lengths in ClO, BrO, and $ClONO_2$,

TABLE 2: Correlation and Basis Set Effects on the Calculated Equilibrium Geometry of $ClONO_2$ (Distances in Ångstroms and Angles in Degrees)

$ClONO_2$	r(Cl−O)	r(O−N)	r(N−O_{cis})	r(N−O_{trans})	α(Cl−O−N)	α(O−N−O_{cis})	α(O−N−O_{trans})
B3LYP/6-311++G(3df)	1.681	1.512	1.184	1.186	113.5	117.2	108.8
MP2/6-311++G(3df)	1.668	1.548	1.185	1.189	111.2	116.3	108.0
experiment[a]	1.673	1.499	1.196	1.196	113.0	118.6	108.8

[a] Ref 32.

TABLE 3: Equilibrium Geometry of ClONO and BrONO Isomers (Distances in Ångstroms and Angles in Degrees)

$ClONO_{cis}$ (Cs)	r(Cl−O)	r(O−N)	r(N−O_{trans})	α(ClON)	α(ONO)
B3LYP/6-311++G(3df)	1.722	1.409	1.160	116.6	117.1
CCSD(T)/TZ2P[a]	1.720	1.489	1.161	113.6	115.6
$ClONO_{trans}$ (Cs)	r(Cl−O)	r(O−N)	r(N−O_{trans})	α(ClON)	α(ONO)
B3LYP/6-311++G(3df)	1.683	1.524	1.145	110.2	108.4
CCSD(T)/TZ2P[a]	1.713	1.542	1.156	107.5	108.1
$BrONO_{cis}$ (Cs)	r(Br−O)	r(O−N)	r(N−O_{trans})	α(BrON)	α(ONO)
B3LYP/6-311++G(3df)	1.922	1.332	1.171	117.9	119.6
CCSD(T)/TZ2P[b]	1.8748	1.4322	1.1710	115.7	116.7
$BrONO_{trans}$ (Cs)	r(Br−O)	r(O−N)	r(N−O_{trans})	α(BrON)	α(ONO)
B3LYP/6-311++G(3df)	1.839	1.498	1.153	111.4	108.3
CCSD(T)/TZ2P[b]	1.8488	1.5285	1.1584	108.4	108.1

[a] Ref 24. [b] Ref 25.

while the MP2 methods somewhat underestimated the same bond lengths. We observe similar behavior in the $BrONO_2$ geometry optimization. The ClO and BrO results are also in excellent agreement with experimental results. The difference between the calculated X−O bond length and the experiment is almost equivalent in ClO and BrO at both the MP2 and the B3LYP levels. In ClO, the Cl−O bond length calculated using MP2 methods is 0.020 Å longer than experimental data, while the B3LYP result is only 0.006 Å longer.

Shown in Table 3 are the equilibrium structures of ClONO and BrONO radicals obtained at the B3LYP/6-311++G(3df) level. Previous theoretical results by Lee are also presented for comparison. Our calculated geometries are generally in good agreement with Lee's results.[24,25] The XO−NO bond lengths calculated using B3LYP/6-311++G(3df) are systematically shorter than Lee's results. Bauerfeldt et al. have calculated the XONO (X = F, Cl, Br) equilibrium structures by using the B3LYP/6-311G(d,p) method. Their geometry parameters of the trans isomer are very close to the results of Lee and the current investigation, but the results are not as satisfactory for the cis isomer. This again indicates that polarization functions play a very important role in the geometry optimization.[34] As mentioned earlier, the XO−NO_2 bond lengths in $ClONO_2$ and $BrONO_2$ from theoretical calculations are all longer than the experimental data. If XONO radicals follow the same trend, shorter XO−NO bond lengths should be expected for XONO radicals. It is difficult to evaluate the accuracy of the two different calculations without knowing the experimental geometry. The bond lengths of X−ONO and XON−O are shorter in the trans isomers than the values in cis isomers for both ClONO and BrONO. This contraction has been attributed to the end X and O atoms interaction by Lee based on his Mulliken population analysis.

Geometry optimizations for NO_2 and NO_3 were also performed at the B3LYP/6-311++G(3df) level of theory although the results are not presented. The ground state geometry of NO_2 and NO_3 has been the object of numerous experimental and theoretical studies. It has been established that the ground state NO_2 has C_{2v} symmetry.[35−39] Although symmetry breaking in NO_2 has been observed at different levels of theory,[39,40] symmetry breaking in NO_2 becomes important only at an ONO angle smaller than 120° where the $^2A_1$ and $^2B_2$ states are coupled, which is far from the experimental equilibrium minimum of the ground state. Therefore, we have constrained the NO_2 geometry to C_{2v} symmetry in our geometry optimization calculation and thereafter the energy calculations. For NO_3, experimental results have strongly indicated D_{3h} symmetry for ground state equilibrium structure of NO_3,[41−43] while different symmetries were found by theoretical studies at different levels of theory.[44−47] Davy and Schaefer's complete active space self-consistent field (CASSCF) calculation with the DZ+P basis set shows that the energy of C_{2v} geometry is 1.4 kcal/mol lower than the D_{3h} geometry.[47] Boehm and Lohr's perturbation theory calculations found that the relative energies of C_{2v} and D_{3h} symmetries depend on the level of theory.[46] Although many experimental results support the D_{3h} symmetry of NO_3 radical, discrepancies still exist. Therefore, Kawaguchi et al. suggested a potential surface of the NO_3 ground state with an overall D_{3h} symmetry and three equivalent C_{2v} minima corresponding to one long N−O bond and two short N−O bond structures.[48] Stanton et al. calculated that the energy difference of D_{3h} and C_{2v} symmetries is about 2.6 kcal/mol, and the barrier height between the equivalent C_{2v} minima is only 0.5 kcal/mol by using the coupled cluster singles and doubles method with quasirestricted Hartree−Fock reference functions (QRHF-CCSD) with the DZP basis set.[49] This potential energy surface model and theoretical calculation are partially supported by the laser-induced fluorescence spectrum of NO_3.[50] Although more theoretical and experimental studies are required to determine the existence of C_{2v} symmetry and the exact energy difference between C_{2v} and D_{3h} symmetries of NO_3, it is clear that this difference will be very small to be consistent with most spectroscopy results. Therefore, the symmetry breaking of NO_3 should only have a minimal effect on our bond energy calculations. Also, the 1.4−2.6 kcal/mol energy difference between C_{2v} and D_{3h} symmetries from theoretical calculations can also be partially compensated by the zero point energy difference of these two symmetries, which is about 2−4 kcal/mol higher for C_{2v} symmetry, due to the symmetry breaking and appearance of higher frequency vibrational modes. Consequently, we have constrained the NO_3 radical to D_{3h} symmetry in our geometry optimization and the energy calculations.

Shown in Table 4 are the harmonic vibrational frequencies without scaling and IR intensities calculated at both MP2 and

TABLE 4: Vibrational Frequencies for $XONO_2$ and XO Where X = Cl and Br

species	mode symmetry	mode no.	mode description[a]	B3LYP/6-311++G(3df)	MP2/6-311++G(3df)	exp[a]
$BrONO_2$	a′	1	NO_2 antisymmetric stretch	1766.34(352)	1907(213)	1714 vs[b]
	a′	2	NO_2 symmetric stretch	1331.91(284)	1301(230)	1288 vs[b]
	a′	3	$ONO_1 + ONO_2$	818.07(196)	780(160)	803.3 vs[b]
	a′	4	BrO stretch + ONO_1-ONO_2 bend	752.73(6.0)	753(41)	750 w[b]
	a′	5	O−N stretch	555.64(101)	503(220)	564 s[b]
	a′	6	ONO_2-ONO_1 bend + BrO stretch	399.23(2.3)	392(46)	394[b]
	a′	7	BrON bend	207.50(0.03)	217(0.4)	
	a″	8	$BrONO_1$ torsion	744.77(9.5)	733(6.1)	728 wm[b]
	a″	9	$BrONO_2$ torsion	123.22(0.19)	116(0.36)	
$ClONO_2$	a′	1	NO_2 a stretch	1797.4(378)	1943(229)	1736.9 vs[c]
	a′	2	NO_2 s stretch	1340.8(269)	1315(214)	1292.84 vs[c]
	a′	3	ClO stretch	828.4(107)	816(22)	809.4 s[c]
	a′	4	mixed	786.6(74)	763(147)	780.22 ms[c]
	a′	5	mixed	562.9(64.8)	527(81)	563.1 s[c]
	a′	6	NO_2 rock	437.5(25.5)	379(140)	434.0 m[c]
	a″	7	ClO rock	249.2(0.16)	256(0.87)	273.3 w[c]
	a″	8	NO_2 wag	731.7(9.7)	716(6.3)	711.0 w[c]
		9	torsion	130.6(0.16)	132(0.37)	120.16[c]
ClO	Sg	1		861.4	852	853.8[d]
BrO	Sg	1		738.91	730	729.9[e]
$ClONO_{trans}$	a′	1	N═O stretch	1849(365)	1800(301)	1752[f]
	a′	2	ONO bend	886(105)	859(39)	
	a′	3	ClO stretch	664(176)	659(217)	
	a′	4	O−N stretch	409(123)	346(201)	
	a′	5	ClON bend	266(0.71)	259(0.08)	
	a″	6		179(0.0075)	173(0.05)	
$ClONO_{cis}$	a′	1	N═O stretch	1758(279)	1793(242)	1715 vs[g]
	a′	2	ONO bend	872(0.81)	841(18)	858 w[g]
	a′	3	ClO stretch	658(63)	688(12)	644 m[g]
	a′	4	O−N stretch	392(84)	280(154)	406 vs[g]
	a′	5	ClON bend	239(0.43)	237(74)	270 T[g]
	a″	6		398(0.99)	337(1.2)	
$BrONO_{trans}$	a′	1	N═O stretch	1820(349)	1773(294)	1723.4 vs [h,I]
	a′	2	ONO deform	869(152)	827(72)	835.9 m[i]
	a′	3	BrO stretch	596(297)	574(282)	586.9 vs[i]
	a′	4	O−N stretch	401(66)	334(198)	391.2 m[i]
	a′	5	torsion	230(0.24)	225(0.18)	150 H[j]
	a″	6		168(0.0079)	163(0.06)	
$BrONO_{cis}$	a′	1	N═O stretch	1700(315)	1662(224)	1650.7 vs[k]
	a′	2	ONO deform	867(12)	862(13)	862.6 w[k]
	a′	3	BrO stretch	720(79)	568(43)	573.5 m[k]
	a′	4	O−N stretch	389(20)	391(209)	420.2 wm[k]
	a′	5		189(0.69)	219(0.06)	
	a″	6		423(1.27)	371(0.88)	

[a] Ref 63. [b] Ref 64. [c] Ref 65. [d] Ref 66. [e] Ref 67. [f] Ref 68. [g] Ref 69. [h] Ref 70. [i] Ref 71. [j] Ref 72. [k] Ref 73.

B3LYP levels of theory with the 6-311++G(3df) basis set for $ClONO_2$, $BrONO_2$, ClO, and BrO. All of the vibrational frequencies refer to ^{79}Br and ^{35}Cl isotopes. The calculated frequencies show only a modest dependence on the computational method for most vibrational modes. In general, both methods reproduce experiment well. The MP2 method overestimates the NO_2 antisymmetric vibrational frequency by as much as 140 cm^{-1} for both $ClONO_2$ and $BrONO_2$.

Overall, we find that the B3LYP/6-311++G(3df) geometries and vibrational frequencies are superior to the MP2/6-311++G(3df) results. These results reinforce the earlier observations that B3LYP geometries are superior to MP2 geometries for these systems.[23] The B3LYP/6-311++G(3df) geometries and harmonic frequencies are used in all energetic calculations in the present work. The bond energy error introduced by differences between the calculated and the experimental vibrational frequencies is expected to be smaller than 1 kcal/mol.

B. Bond Dissociation Energies. A methodology similar to that previously used in our laboratory was chosen for the energy calculations.[51] Because accurate ab initio calculations of compounds containing elements from the second and third rows of the periodic table can be a formidable task even with high-performance computers, McGivern et al. have developed correction factors for basis set effects and correlation effects. We also have applied correction factors for the zero point energies, the spin−orbit energy of the atomic and diatomic fragments, and finally the thermal corrections in order to compare with experimental results. All calculations were performed using Gaussian 94[52] or 98.[53] The MP2 and CCSD(T) calculations were performed by correlating only the valence electrons (frozen core approximation). For N, O, 1s-like core molecular orbitals, for Cl 1s and 2sp-like core molecular orbitals, and for Br, 1s, 2sp, and 3spd-like core molecular orbitals were constrained to be doubly occupied, unless noted otherwise. Representative results are shown for the $ClO-NO_2$ and $(ClONO)_{trans}-O$ bond dissociation energies of $ClONO_2$ in Figures 1 and 2, respectively. One of the advantages of the correlation consistent basis sets is that the energy change with increasing basis set size can be accurately modeled.[30,54,55] After the basis set is increased, the energies smoothly approach the asymptotic infinite basis set limit. Therefore, the bond energies in the infinite basis set limit can be obtained by simply extrapolating the MP2/cc-pVXZ (X = 2−5) to infinity by using the appropriate functional form. Although many functional forms

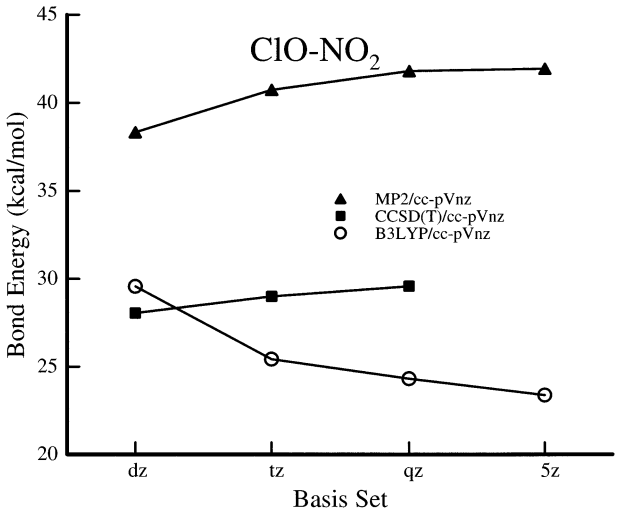

Figure 1. Correlation and basis set effects of $ClO-NO_2$ bond energy calculation. The MP2 and CCSD(T) results have different basis set dependencies as compared to B3LYP results. All of the bond energies shown in the figure are raw energies without any corrections that correspond to the D_{raw} term in eq 6 (this is the same as in Figures 2−5).

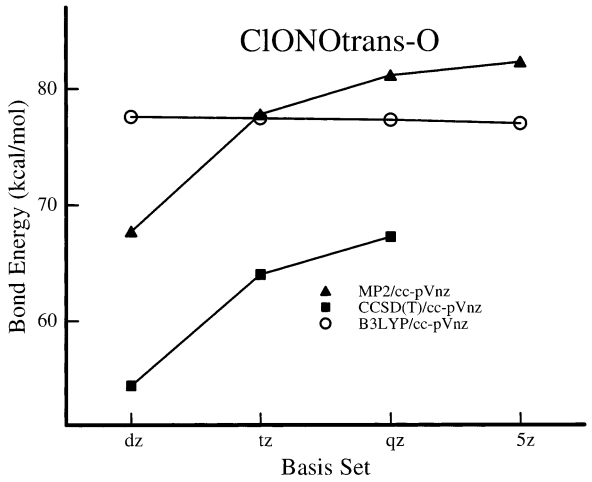

Figure 2. Correlation and basis set effects of $(ClONO)_{trans}-O$ bond energy calculation.

can be used for this extrapolation, we have selected the exponential function (4) and the polynomial function (5), where X indicates the size of the basis set size (cc-pVXZ). Three parameters are required in both functions

$$E(\mathrm{X}) = A_0 + A_1 \exp(-A_2\mathrm{X}) \quad (4)$$

$$E(\mathrm{X}) = A_0 + \frac{A_1}{\mathrm{X}^3} + \frac{A_2}{\mathrm{X}^5} \quad (5)$$

and A_0 represents the asymptotic basis set limit. The raw MP2/cc-pVXZ electronic energies for each species were fitted by either function using the nonlinear least-squares regression method. The complete basis set limit electronic energies for each species are estimated this way and are used to calculate the basis set limit bond energies. Instead of fitting each raw energy curve, one can alternatively fit the bond energy curve to approximate the infinite basis set limit bond energies. If a polynomial function is used, there is no difference between the fitted raw energy curve and the fitted bond energy curve since the bond energy is a linear combination of the raw energy and linear combination of polynomial is still polynomial of the same order. However, for exponential functions, there will be some difference if the fitting sequence is different and this difference will depend on the curvature of the energies. In the case of the $ClONO_2$ bond energy calculations, this difference is small. For $BrONO_2$, the difference is large enough to cause problems in the extrapolation procedure. Therefore, we have not applied the extrapolation method for $BrONO_2$ and used the MP2/cc-pV5Z value instead. All of the raw energies at the MP2 and CCSD(T) levels of theory are listed in Tables 8 and 9.

To compare with experimental values, the 298 K CCSD(T) basis set limit bond enthalpies were calculated by using the following equation

$$D_0^{298\mathrm{K}} = D_{raw} + \Delta E_{ZPE} + \Delta E_{spin} + \Delta E_{298\mathrm{K}} + \Delta E_{corr} \quad (6)$$

where D_{raw} is bond energy calculated by using the basis set limit electronic energies of the reactant and products from the extrapolation without any correction factors applied on it, ΔE_{ZPE} is the zero point energy correction, ΔE_{spin} is the spin−orbit coupling correction, ΔE_{298K} is the correction for 298 K, and ΔE_{corr} is the correlation correction of MP2 bond energy.

Recent studies on the bond dissociation energies of HX and X_2 (X = F, Cl, Br, and I) have shown that the spin−orbit energy of the atomic halogen fragment represents the major difference between the relativistic and the nonrelativistic treatments.[56,57] Therefore, we have chosen to apply an atomic spin−orbit correction defined as one-third of the known experimental spin−orbit energy for each halogen atom. This correction represents the statistical weighted average of the relative energies of the 4-fold degenerate $^2P_{3/2}$ and the higher-energy doubly degenerate $^2P_{1/2}$ electronic states. The correction decreases the calculated nonrelativistic bond energy to correctly model the dissociation on the ground state potential energy surface to give $X(^2P_{3/2})$ products (X = Cl and Br). The relativistic corrections were also extended to the O atom and ClO and BrO radicals by assuming that the spin−orbit energies are still the major relativistic corrections. For these species, this correction is not as significant due to the small splitting between the submagnetic levels. The value of $\langle S^2 \rangle$ was less than 0.775 before annihilation for all open shell species studied, and the effects of spin contamination on the calculated bond dissociation energy are expected to be small.

The effect of electron correlation on the bond dissociation energy was taken into account by comparing MP2 and CCSD(T) results calculated with identical basis sets. It can be seen from Figure 1 that higher levels of correlation decrease the bond dissociation energy, and with a basis set beyond cc-pVTZ, the changes are almost identical to that of the cc-pVTZ difference. McGivern et al. have reported that correlation corrections are almost constant from cc-pVTZ to cc-pV5z in their C−X (X = Cl, Br) bond energy calculation,[51] and we have assumed that the cc-pVTZ correlation correction remains unchanged up to the basis set limit. By applying this correlation correction to the MP2 basis set limit bond energies, the CCSD(T) basis set limit bond energies can be derived.

B3LYP/6-311++G(3df) zero point energy corrections were also included in the bond dissociation energy calculations. Table 5 shows the results of these calculations along with the experimental bond dissociation energies for ClO and $ClONO_2$. When direct measurements of bond dissociation energies were not available, the experimental values were derived from available standard enthalpies of formation at 298 K. Thermodynamic values were typically taken from the most recent review of thermodynamic data available.[58,59] No error bars were associated with enthalpies of formation taken from ref 59, so

TABLE 5: $ClONO_2$ and ClO Bond Dissociation Energies

bond	MP2/CBL_a bond energy[a]	MP2/CBL_b bond energy[b]	atomic spin−orbit correction	correlation correction	ZPC	$D_0^{298} - D_0^0$	corrected bond enthalpy at 298 K CBL_a	corrected bond enthalpy at 298 K CBL_b	exp
ClO									
Cl−O	63.43	64.67	−0.576	−0.30	−1.2314	0.89	62.21	63.45	63.31 [c]
$ClONO_2$									
$Cl-ONO_2$	42.64	41.79	−0.8	2.98	−3.18	0.83	42.47	41.62	41.73
$ClO-NO_2$	42.83	42.20	−0.303	−11.74	−3.06	0.91	28.64	28.01	26.8
$(ClONO)_{cis}-O$	83.53	83.76	−0.079	−13.80	−3.68	1.33	67.21	67.54	69.47 [d]
$(ClONO)_{trans}-O$	90.06	90.17	−0.079	−14.30	−3.98	1.42	73.12	73.23	72.07 [d]

[a] The value is obtained by using exponential function. [b] The value is obtained by using polynomial function. [c] Ref 74. [d] Because no experimental values are available for heats of formation enthalpies for ClONO isomers, these values are taken from Lee's theoretical calculation in ref 24.

TABLE 6: $BrONO_2$ and BrO Bond Dissociation Energies

bond	MP2/cc-PV5Z	atomic spin−orbit correction	correlation correction	zero point correction	$D_0^{298} - D_0^0$	corrected bond dissociation energy	exp
BrO							
Br−O	54.82	−1.865	1.84	−1.036	0.159	53.918	55.36[a]
$BrONO_2$							
$Br-ONO_2$	37.78	−3.5	3.78	−2.945	0.77	35.89	34.9
$BrO-NO_2$	46.05	−0.857	−13.07	−3.017	0.83	29.94	28.2 ± 1.5[b]
$(BrONO)_{cis}-O$	82.17	−0.079	−13.70	−3.446	1.26	66.21	68.0[c]
$(BrONO)_{trans}-O$	84.21	−0.079	−12.81	−3.741	1.61	69.19	71.9[c]

[a] Ref 74. [b] Ref 19. [c] Because no experimental values are available for heats of formation enthalpies for BrONO isomers, these values are taken from Lee's theoretical calculation in ref 25.

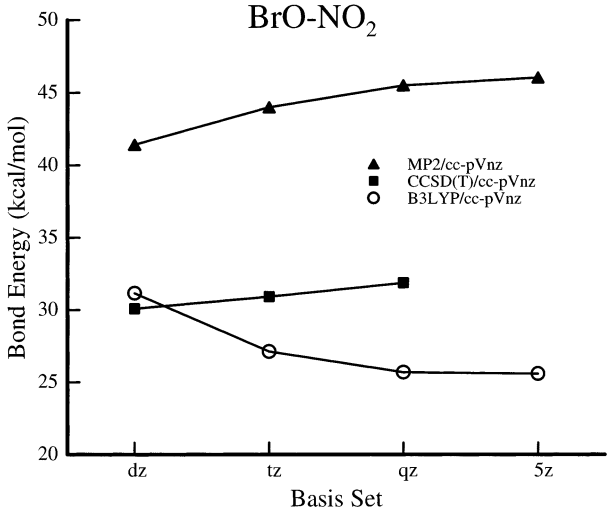

Figure 3. Correlation and basis set effects of $BrO-NO_2$ bond energy calculation.

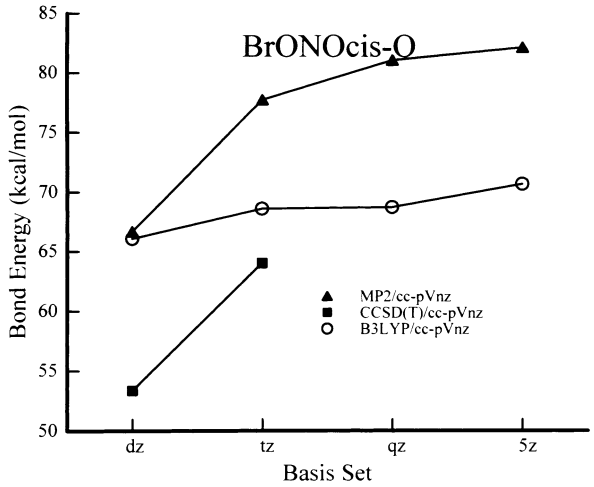

Figure 4. Correlation and basis set effects of $(BrONO)_{cis}-O$ bond energy calculation.

no error bars are given for experimental bond dissociation energies that were calculated from these enthalpies. However, we estimate that the error is on the order of 1−2 kcal/mol, based on previously published values. Although the calculated values using both exponential and polynomial functions agree remarkably well with experiment, it is clear that the polynomial function predicts more accurate values as compared to experimental data, differing by less than 1.2 kcal/mol for Cl−O, $Cl-ONO_2$, and $ClO-NO_2$ bond dissociation energies (Table 5). Because there are no experimental values available for ClONO isomers, the experimental value of (ClONO)−O bonds is obtained with the known heat of formation of $ClONO_2$ and O with the calculated heat of formation of ClONO radicals by Lee.[24] Among all of the bonds, the $ClO-NO_2$ bond is the weakest, and the (ClONO)−O bonds are the strongest. We find an approximately 6 kcal/mol (ClONO)−O bond energy difference between the cis and the trans ClONO isomers. The experimental value listed in Table 5 for the $(ClONO)_{cis}-O$ bond energy is 2 kcal/mol higher than our results, and $(ClONO)_{trans}-O$ is 1 kcal/mol lower than our result. Our calculated (ClONO)−O bond energies agree well with the derived experimental values, indicating that the accuracy of the extrapolation methods is comparable to Lee's CCSD(T)/ANO results.

Correction factors for $BrONO_2$ bond energies were determined following a similar procedure as for the $ClONO_2$ bond energies (Table 6). Representative results of $BrO-NO_2$ and $(BrONO)_{cis}-O$ bond energies are shown in Figures 3 and 4. Correlation effects were determined by calculating the difference between MP2/cc-pVTZ and CCSD(T)/cc-pVTZ bond dissociation energies. The basis set-dependent bond energies are shown in Figure 3 for BrO and $BrONO_2$. The cc-pVDZ up to cc-pVQZ basis sets were used for CCSD(T) energy calculations. It can be seen from the figure that correlation differences between MP2 and CCSD(T) calculations remain constant from the cc-pVTZ basis set to the larger basis sets. The correction factors and zero point-corrected bond dissociation energies for the $BrONO_2$ species are shown in Table 6. Instead of extrapolating the energy

TABLE 7: Bond Energies for NO_3, ClONO, and BrONO

bond	MP2/cc-PV5Z	atomic spin−orbit correction	correlation correction	ZPC	$D_0^{298} - D_0^0$	corrected bond dissociation energy	exp
NO_3							
$O-NO_2$	63.02	−0.079	−15.0	−1.108	0.84	47.67	48.69
ClONO							
$Cl-ONO_{cis}$	22.35	−0.8	1.76	−0.61	0.45	23.15	
$Cl-ONO_{trans}$	15.76	−0.8	2.26	−0.31	0.36	17.27	
$ClO-NO_{cis}$	46.51	−0.3	−11.54	−2.07	0.91	33.51	
$ClO-NO_{trans}$	39.91	−0.3	−11.04	−1.78	0.91	27.7	
Br−ONO							
$Br-ONO_{cis}$	18.63	−3.5	2.47	−0.61	0.48	17.47	
$Br-ONO_{trans}$	16.56	−3.5	1.58	−0.31	0.31	14.64	
$BrO-NO_{cis}$	50.71	0.86	−12.96	−1.66	1.67	38.62	
$BrO-NO_{trans}$	48.65	0.86	−13.86	−2.77	1.67	34.55	

to infinite basis set limit, the effective CCSD(T)/cc-pV5z bond energies were calculated. The corrected bond energies of Br−O, $Br-ONO_2$, and $BrO-NO_2$ agree well with the experimental value within ∼2 kcal/mol.

Experimental studies of the thermal dissociation of $BrONO_2$ have shown that since the $BrO-NO_2$ bond is the weakest in the molecule, the dominant products of thermal dissociation are BrO and NO_2. The Br + NO_3 dissociation channel is almost negligible at room temperature. We performed variational transition state theory (vTST) calculations to determine the dissociation rate constant for the BrO + NO_2 channel in order to assess the accuracy of our reported bond energy. The unscaled B3LYP/6-311++G(3df) frequencies and geometries are used to calculate the partition function for parent and products. An exponential decay model for treating the disappearing vibrational modes and to connect conserved reactant and product vibrational frequencies was assumed.[60] The transition state was located by finding the minimum flux on a Morse potential. To reproduce the thermal dissociation rates of $BrONO_2$ reported by Orlando and Tyndall[19] and bimolecular association reaction rates of BrO + NO_2 by Thorn et al.,[61] the $BrO-NO_2$ bond energy should be ≤29 kcal/mol, which is slightly lower than our calculated value. The theoretical heats of formation of BrONO isomers calculated by Lee[25] are adopted to obtain the experimental values of (BrONO)−O bond energies in Table 6. The calculated $(BrONO)_{cis}-O$ bond energy is 1.8 kcal/mol higher than the experimental value, and the calculated $(BrONO)_{trans}-O$ bond energy is 2.8 kcal/mol higher than the experimental result. Because the heat of formation of the O atom has been accurately determined, and the heat of formation of $BrONO_2$ has also been measured by Orlando and Tyndall[19] with high accuracy, we attribute the difference to the uncertainties in the heats of formation of BrONO isomers. Further experimental studies are needed to elucidate this discrepancy.

Calculations of NO_3, ClONO, and BrONO Bond Energies. In addition to the bond energies of $ClONO_2$ and $BrONO_2$, the bond energies of $O-NO_2$, Cl−ONO, Br−ONO, ClO−NO, and BrO−NO were also calculated following the same methodology as an indicator of the performance and the results are given in Table 7. Only the $O-NO_2$ bond energies are shown in Figure 5. We find that the NO_3 bond energy is 1.2 kcal/mol lower than experimental results. On the basis of heats of formation values for O, $ClONO_2$, and $BrONO_2$, we estimate heats of formation of 13.8 and 19.9 kcal/mol for ClONO cis and trans isomers and 16.8 and 19.8 kcal/mol for BrONO cis and trans isomers, respectively. The bond energy calculations show that for both cis and trans conformers, the X−ONO bonds are about 10 kcal/mol weaker than the XO−NO bond. Because dissociation through X + ONO and XO + NO is all simple bond rupture reactions, it is reasonable to assume that both reactions will have loose transition states. Therefore, the dominant secondary dissociation of XONO will be X + ONO in $XONO_2$ photodissociation, which produces XONO (pathway 3) with internal energy near the dissociation threshold. The overall reaction, therefore, would result in identical products to initial $X-ONO_2$ bond cleavage followed by NO_3 secondary dissociation. However, if XONO is produced with very high internal energies, the contribution from XO + NO may not be negligible.

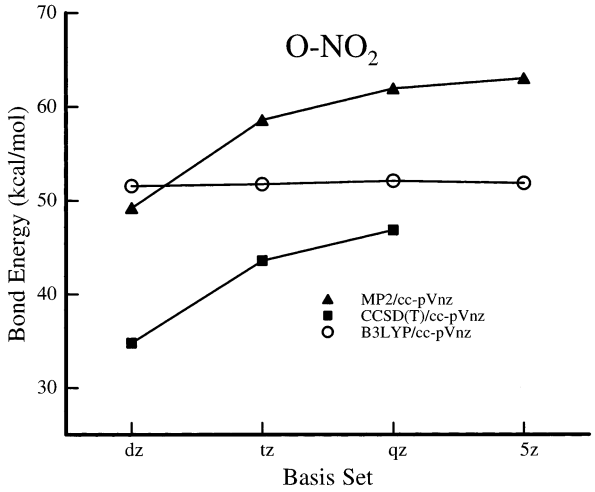

Figure 5. Correlation and basis set effects of $O-NO_2$ bond energy calculation.

Bond Energies Using Density Functional Methods. In addition to MP2 and CCSD(T) calculations, we performed calculations using DFT (B3LYP) with cc-pVXZ basis sets to determine bond energies in ClO, $ClONO_2$, BrO, and $BrONO_2$. The density functional methods have been demonstrated that they are effective at reproducing many molecular properties of bromine compounds.[23] However, the accuracy of bond energy calculations using density functional methods is still debatable especially for processes involving radicals.

As shown in Figures 1−5, the B3LYP method results exhibit a different basis set dependence as compared to MP2 and CCSD(T) values. The B3LYP method consistently underestimates the bond energies associated with closed shell molecules ($XONO_2$), while overestimating the bond energies in open shell radicals (XO). In NO_3, the bond energy is in good agreement with both CCSD(T) and experimental results. Lazarou et al. have performed an extensive series of calculations on the bond dissociation energies of halogenated molecules using DFT methods.[62] The authors have found that the accuracy of bond energies can be improved significantly by empirically increasing the radical electronic energies by an amount relative to the total electron number in the radical. This observation can partially

explain the underestimation of the bond energies of close shell molecules, and the closeness of bond energies for $O-NO_2$ between DFT and CCSD(T) calculations, but cannot explain the overestimation of bond energies in X−O radicals. On the basis of the intrinsic characteristics of electronic correlation behavior, a nonlinear dependence of DFT energy correction is expected. Therefore, for larger radicals, the correction of DFT methods will be larger than the value predicted by assuming a linear dependency. For the $O-NO_2$ bond, because the electron number of the system is relatively small, the B3LYP can still well predict the bond energies, while for X−O molecules, the nonlinear effects are expected to be much larger. With limited results, the nonlinear effects for radicals still require more evidence. We anticipate similar effects on X−ONO bond energy calculations with DFT methods.

III. Summary

The bond dissociation energies of $ClONO_2$ and $BrONO_2$ bonds were determined using correlation consistent (cc-pVXZ) basis sets at MP2 and CCSD(T) levels of theory through a general methodology developed to correct MP2/cc-pVTZ calculations for basis set and electron correlation effects. The fully corrected energies reproduce the experimental values extremely well in most cases.

Acknowledgment. We thank Dr. Michael B. Hall, Dr. David F. Feller, and David E. Woon for helpful discussions. Hardware and software support from the Texas A&M University Supercomputing Facility and the Texas A&M University Laboratory for Molecular Simulations under the National Science Foundation Grant No. CHE-9528196 is acknowledged. S.W.N. also acknowledges support from a Texas Research Enhancement Grant.

Supporting Information Available: Bond energy calculations of the raw energies of $ClONO_2$ and $BrONO_2$ using the MP2, CCSD(T), and B3LYP methods. The material is available free of charge via the Internet at http://pubs.acs.org.

References and Notes

(1) Rowland, F. S.; Spencer, J. E.; Molina, M. J. *J. Phys. Chem*. **1976**, *80*, 2711.
(2) Spencer, J. E.; Rowland, F. S. *J. Phys. Chem*. **1978**, *82*, 7.
(3) Solomon, S.; Mills, M.; Heidt, L. E.; Pollock, W. H.; Tuck, A. F. *J. Geophys. Res.* **1992**, *97*, 25.
(4) Garcia, R. R.; Solomon, S. *J. Geophys. Res*. **1994**, *99*, 12937.
(5) Minton, T. K.; Nelson, C. M.; Moore, T. A.; Okumura, M. *Science* **1992**, *258*, 1342.
(6) Nelson, C. M.; Moore, T. A.; Okumura, M.; Minton, T. K. *Chem. Phys*. **1996**, *207*, 287.
(7) Goldfarb, L.; Schmoltner, A.; Gilles, M. K.; Burkholder, J. B.; Ravishankara, A. R. *J. Phys. Chem. A* **1997**, *101*, 6658.
(8) Yokelson, R. J.; Burkholder, J. B.; Fox, R. W.; Ravishankara, A. R. *J. Phys. Chem. A* **1997**, *101*, 6667.
(9) Harwood, M. H.; Burkholder, J. B.; Ravishankara, A. R. *J. Phys. Chem. A* **1998**, *102*, 1309.
(10) Chang, J. S.; Barker, J. R.; Davenport, J. E.; Golden, D. M. *Chem. Phys. Lett.* **1979**, *60*, 385.
(11) Margitan, J. J.; Johnston, H. S. *Chem. Phys. Lett*. **1982**, *93*, 127.
(12) Zou, P.; Park, J.; Schmitz, B. A.; Nguyen, T.; North, S. W. *J. Phys. Chem. A* **2002**, *106*, 1004.
(13) Knauth, H. D.; Martin, H.; Stockmann, W. *Z. Naturforsch*. **1974**, *29a*, 200.
(14) Alqasmi, R.; Knauth, H.-D.; Rohlack, D. *Ber. Bunsen-Ges. Phys. Chem*. **1978**, *82*, 217.
(15) Schonle, G.; Knauth, H. D.; Schindler, R. M. *J. Phys. Chem*. **1979**, *83*, 3297.
(16) Patrick, R.; Golden, D. M. *Int. J. Chem. Kinet.* **1983**, *15*, 1189.
(17) Handwerk, V.; Zellner, R. *Ber. Bunsen-Ges. Phys. Chem*. **1984**, *88*, 405.
(18) Anderson, L. C.; Fahey, D. W. *J. Phys. Chem*. **1990**, *94*, 644.
(19) Orlando, J. J.; Tyndall, G. S. *J. Phys. Chem.* **1996**, *100*, 19398.
(20) DeMore, W. B.; Sander, S. P.; Golden, D. M.; Hampson, R. F.; Kurylo, M. J.; Howard, C. J.; Ravishankara, A. R.; Kolb, C. E.; Molina, M. J. *Chemical Kinetics and Photochemical Data for Use in Stratospheric Modeling*; Evaluation Number 11; NASA JPL Publications: 1994; No. 94-26.
(21) Lee, T. J. *J. Phys. Chem.* **1995**, *99*, 1943.
(22) Parthiban, S.; Lee, T. J. *J. Chem. Phys*. **1998**, *109*, 525.
(23) Parthiban, S.; Lee, T. J. *J. Chem. Phys*. **2000**, *113*, 145.
(24) Lee, T. J. *J. Phys. Chem*. **1994**, *98*, 111.
(25) Lee, T. J. *J. Phys. Chem*. **1996**, *100*, 19847.
(26) Hohenberg, P.; Kohn, W. *Phys. Rev. B* **1964**, *136*, 864.
(27) Becke, A. D. *J. Chem. Phys*. **1993**, *98*, 5648.
(28) Krishnan, R.; Binkley, J. S.; Seeger, R.; Pople, J. A. *J. Chem. Phys.* **1980**, *72*, 650.
(29) Mclean, A. D.; Chandler, G. S. *J. Chem. Phys*. **1980**, *72*, 5639.
(30) Dunning, T. H., Jr. *J. Chem. Phys.* **1989**, *90*, 1007.
(31) Woon, D. E.; Dunning, T. H., Jr. *J. Chem. Phys.* **1993**, *98*, 1358.
(32) Casper, B.; Lambotte, P.; Minkvitz, R.; Oberhammer, H. *J. Phys. Chem*. **1993**, *97*, 9992.
(33) Ying, L.; Zhao, X. *J. Phys. Chem*. **1997**, *101*, 3569.
(34) Bauerfeldt, G. F.; Arbilla, G.; da Silva, E. C. *J. Mol. Struct*. **2001**, *539*, 223.
(35) Hardwick, J. L.; Brand, J. C. D. *Can. J. Phys*. **1976**, *54*, 80.
(36) Morino, Y.; Tanimoto, M.; Saito, S.; Hirota, E.; Awata, R.; Tanaka, T. *J. Mol. Spectrosc*. **1983**, *98*, 331.
(37) Xie, Y.; Davy, R. D.; Yates, B. F.; Blahous, C. P. B.; Yamaguchi, Y.; Schaefer, H. F., III. *J. Chem. Phys.* **1989**, *135*, 179.
(38) Kaldor, U. *Chem. Phys. Lett*. **1990**, *170*, 17.
(39) Blahous, C. P., III; Yates, B. F.; Xie, Y.; Schaefer, H. F., III. *J. Chem. Phys.* **1990**, *93*, 8105.
(40) Jackels, C. F.; Davidson, E. R. *J. Chem. Phys*. **1976**, *64*, 2908.
(41) Weaver, A.; Arnold, D. W.; Bradforth, S. E.; Neumark, D. M. *J. Chem. Phys.* **1991**, *94*, 1740.
(42) Hirota, E.; Kawaguchi, K.; Ishiwata, T.; Tanaka, I. *J. Chem. Phys*. **1991**, *95*, 771.
(43) Fiedl, R. R.; Sander, S. P. *J. Phys. Chem.* **1987**, *91*, 2721.
(44) Kaldor, U. *Chem. Phys. Lett*. **1991**, *185*, 131.
(45) Siegbahn, P. E. M. *J. Comput. Chem*. **1985**, *6*, 182.
(46) Boehm, R. C.; Lohr, L. L. *J. Phys. Chem*. **1989**, *93*, 3430.
(47) Davy, R. D.; Schaefer, H. F., III. *J. Chem. Phys*. **1989**, *91*, 4410.
(48) Kawaguchi, K.; Hirota, E.; Ishiwata, T.; Tanaka, I. *J. Chem. Phys*. **1990**, *93*, 951.
(49) Stanton, J. F.; Gauss, J.; Bartlett, R. *J. Chem. Phys*. **1991**, *94*, 4084.
(50) Kim, B.; Hunter, P. L.; Johnston, H. S. *J. Chem. Phys*. **1992**, *96*, 4057.
(51) McGivern, W. S.; Derecskei-Kovac, A.; North, S. W. *J. Phys. Chem. A* **2000**, *104*, 436.
(52) Frisch, M. J.; Trucks, G. W.; Schlegel, H. B.; Gill, P. M. W.; Johnson, B. G.; Robb, M. A.; Cheeseman, J. R.; Keith, T.; Petersson, G. A.; Montgomery, J. A.; Raghavachari, K.; Al-Laham, M. A.; Zakrzewski, V. G.; Ortiz, J. V.; Foresman, J. B.; Cioslowski, J.; Stefanov, B. B.; Nanayakkara, A.; Challacombe, M.; Peng, C. Y.; Ayala, P. Y.; Chen, W.; Wong, M. W.; Andres, J. L.; Replogle, E. S.; Gomperts, R.; Martin, R. L.; Fox, D. J.; Binkley, J. S.; Defrees, D. J.; Baker, J.; Stewart, J. P.; Head-Gordon, M.; Gonzalez, C.; Pople, J. A. *Gaussian 94*, revision D.4; Gaussian, Inc.: Pittsburgh, PA, 1995.
(53) Frisch, M. J.; Trucks, G. W.; Schlegel, H. B.; Scuseria, G. E.; Robb, M. A.; Cheeseman, J. R.; Zakrzewski, V. G.; Montgomery, J. A., Jr.; Stratmann, R. E.; Burant, J. C.; Dapprich, S.; Millam, J. M.; Daniels, A. D.; Kudin, K. N.; Strain, M. C.; Farkas, O.; Tomasi, J.; Barone, V.; Cossi, M.; Cammi, R.; Mennucci, B.; Pomelli, C.; Adamo, C.; Clifford, S.; Ochterski, J.; Petersson, G. A.; Ayala, P. Y.; Cui, Q.; Morokuma, K.; Malick, D. K.; Rabuck, A. D.; Raghavachari, K.; Foresman, J. B.; Cioslowski, J.; Ortiz, J. V.; Stefanov, B. B.; Liu, G.; Liashenko, A.; Piskorz, P.; Komaromi, I.; Gomperts, R.; Martin, R. L.; Fox, D. J.; Keith, T.; Al-Laham, M. A.; Peng, C. Y.; Nanayakkara, A.; Gonzalez, C.; Challacombe, M.; Gill, P. M. W.; Johnson, B. G.; Chen, W.; Wong, M. W.; Andres, J. L.; Head-Gordon, M.; Replogle, E. S.; Pople, J. A. *Gaussian 98*, revision A.6; Gaussian, Inc.: Pittsburgh, PA, 1998.
(54) Davidson, E. R.; Feller, D. *Chem. Rev*. **1986**, *86*, 681.
(55) Dunning, T. H., Jr. *J. Phys. Chem. A* **2000**, *104*, 9062.
(56) Visscher, L.; Dyall, K. G. *J. Chem. Phys.* **1996**, *104*, 9040.
(57) Visscher, L.; Styszynski, J.; Nieuwpoort, W. C. *J. Chem. Phys.* **1996**, *105*, 1987.
(58) Zhang, Z.; Pollard, R. *Thermochim. Acta* **1995**, *257*, 21.
(59) Chase, M. W. NIST-JANAF Themochemical Tables, Fourth Edition. *J. Phys. Chem. Ref. Data* **2001**, Monograph 9, 1−1951.
(60) Hase, W. L. *Chem. Phys. Lett.* **1987**, *139*, 389.
(61) Thorn, R. P.; Daykin, E. P.; Wine, P. H. *Int. J. Chem. Kinet*. **1993**, *25*, 521.
(62) Lazarou, T. G.; Prosmitis, A. V.; Papadimitriou, V. C.; Papagiannakopoulos, P. *J. Phys. Chem. A* **2001**, *105*, 6729.

(63) Shimanouchi, T. Molecular Vibrational Frequencies. In *NIST Chemistry WebBook*; NIST Standard Reference Database Number 69; Linstrom, P. J., Mallard, W. G., Eds.; National Institute of Standards and Technology: Gaithersburg, MD, July 2001; (http://webbook.nist.gov).
(64) Wilson, W. W.; Christe, K. O. *Inorg. Chem.* **1987**, *26*, 1573.
(65) Orphal, J.; Morillon-Chapey, M.; Diallo, A.; Guelachvili, G. *J. Phys. Chem. A* **1997**, *101*, 10062.
(66) Amano, T.; Saito, S.; Hirota, E.; Morino, Y. J. *Mol. Spectrosc.* **1969**, *30*, 275.
(67) Amano, T.; Yoshinaga, A.; Hirota, E. *J. Mol. Spectrosc.* **1972**, *44*, 594.
(68) Tevault, D. E.; Smardzewski, R. R. *J. Chem. Phys.* **1977**, *67*, 3777.
(69) Janowski, B.; Knauth, N.-D.; Martin, H. *Ber. Bunsen-Ges. Phys. Chem.* **1977**, *81*, 1262.
(70) Feuerhahn, M.; Minkwitz, R.; Engelhardt, U. *J. Mol. Spectrosc.* **1979**, *77*, 429.
(71) Tevault, D. E. *J. Phys. Chem.* **1979**, *83*, 2217.
(72) Scheffler, D.; Grothe, H.; Willner, H.; Frenzel, A.; Zetsch, C. *Inorg. Chem.* **1997**, *36*, 335.
(73) Scheffler, D.; Willner, H. *Inorg. Chem.* **1998**, *37*, 4500.
(74) Durie, R. A.; Ramsay, D. A. *Can. J. Phys.* **1958**, *36*, 35.